Ozone Formation in Ternary Collisions: Theory and Experiment Reconciled

Marjan Mirahmadi,[1] Jesús Pérez-Ríos,[1,2] Oleg Egorov,[3] Vladimir Tyuterev,[3,4] and Viatcheslav Kokoouline[5]
[1]Fritz-Haber-Institut der Max-Planck-Gesellschaft, Faradayweg 4-6, 14195 Berlin, Germany
[2]Department of Physics and Astronomy, Stony Brook University, Stony Brook, New York 11794, USA
[3]Quamer Laboratory, Tomsk State University, 634050 Tomsk, Russia
[4]Groupe de Spectrometrie Moléculaire et Atmospherique, UMR CNRS 7331, University of Reims Champagne-Ardenne, 51687 Reims, France
[5]Department of Physics, University of Central Florida, Florida 32816, USA

(Received 8 October 2021; revised 24 December 2021; accepted 28 January 2022; published 10 March 2022)

The present Letter shows that the formation of ozone in ternary collisions $O + O_2 + M$—the primary mechanism of ozone formation in the stratosphere—at temperatures below 200 K (for $M = Ar$) proceeds through a formation of a temporary complex MO_2, while at temperatures above ~700 K, the reaction proceeds mainly through a formation of long-lived vibrational resonances of O_3^*. At intermediate temperatures 200–700 K, the process cannot be viewed as a two-step mechanism, often used to simplify and approximate collisions of three atoms or molecules. The developed theoretical approach is applied to the reaction $O + O_2 + Ar$ because of extensive experimental data available. The rate coefficients for the formation of O_3 in ternary collisions $O + O_2 + Ar$ without using two-step approximations were computed for the first time as a function of collision energy. Thermally averaged coefficients were derived for temperatures 5–900 K. It is found that the majority of O_3 molecules formed initially are weakly bound. Accounting for the process of vibrational quenching of the nascent population, a good agreement with available experimental data for temperatures 100–900 K is obtained.

DOI: 10.1103/PhysRevLett.128.108501

Introduction.—Being the major absorber of the UV light in the upper atmosphere [1], the ozone molecule is crucial for the well being of humanity. However, the tropospheric ozone, the concentration of which near the Earth's surface was doubled or tripled in the troposphere during the 20th century [2] is harmful to the human respiratory system and, therefore, is considered as an air pollutant. Therefore, from an ecological point of view, ozone should be protected from destruction in the upper atmosphere, but its production in living or working spaces must be minimized. Furthermore, the O_3/O_2 photochemical cycle has a significant impact on the chemistry in the Earth's atmosphere and climate change [3]. However, despite its importance and decades of research, the reaction leading to ozone formation is not fully understood due to its complexity.

In Earth's ionosphere, formation of ozone occurs through the reaction of ternary recombination: $O_2 + O + M \rightarrow O_3 + M$, where M is typically N_2 or O_2. Knowledge of the "nascent population" of ozone is essential for reliable modeling of the satellite measurements in nonlocal thermodynamic conditions of the upper atmosphere [4–6]. In many laboratory experiments [7–10] it was shown that the ternary rate coefficient k_3 for $M = N_2$ have a very similar behavior as those of $M = Ar$. A complete database is available [9] for the argon colliding partner, which is thus often used to study ozone formation.

In the existing literature, two simplified mechanisms were proposed to analyze the process. Both mechanisms proceed in two steps forming an intermediate complex: stabilization and Chaperon mechanisms. In the stabilization mechanism (also known as energy transfer mechanism), the complex is a long-lived rovibrational resonance O_3^* of ozone, whereas, in the Chaperon mechanism, the complex is a resonance of O_2M^*. Consequently, at given conditions, ozone formation would be dominated by one of these mechanisms depending on the partial pressures of the colliding species. However, using the results from a *direct* ternary recombination approach, i.e., without invoking the formation of an intermediate complex, may help to clear up the dilemma revealing the role of each of the mechanisms at a given density.

In this Letter, we present a *direct* three-body recombination approach to studying the formation of ozone without invoking the formation of an intermediate complex. The present theoretical approach combines an *ab initio* potential energy surface (PES) of the ArO_3 system, obtained in this Letter, and the classical-trajectory method

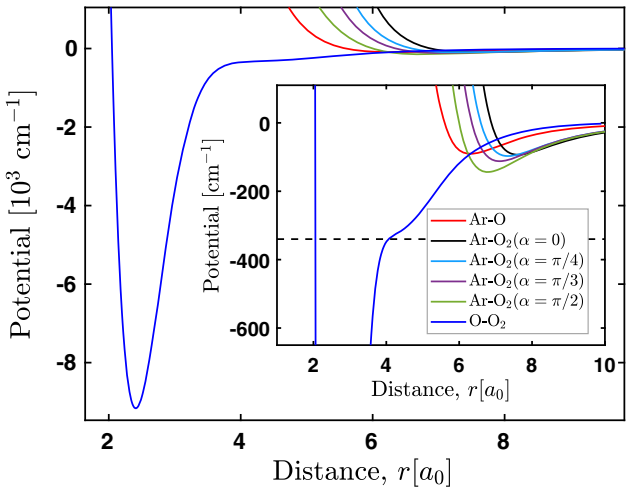

FIG. 1. Relevant interaction potentials for the reaction $O_2 + O + Ar \rightarrow O_3 + Ar$. The O_2-O curve shows the minimum energy path for dissociation of ozone [14]. Dissociation energies are $D_e^{O-O_2} = 9164$ cm^{-1} ($\approx 1.5 \times 10^4$ K) and $D_e^{Ar-O} = 90.7967$ cm^{-1} (≈ 131 K). The angle α describes the orientation of the O_2 axis with respect to direction towards to Ar. For for $\alpha = 0$, $D_e^{Ar-O_2} = 93.13$ cm^{-1} (≈ 134 K) and for $\alpha = \pi/2$, $D_e^{Ar-O_2} = 143.6462$ cm^{-1} (≈ 207 K). The black dashed line in the inset indicates the energy of the shoulder structure of $O - O_2$ at ≈ 340 cm^{-1} (≈ 489 K).

in hyperspherical coordinates developed previously by two of us [11–13].

ArO_3 *potential.*—The potential energy surface (PES) used in this Letter is constructed as the sum $V = V_{O-O_2} + V_{Ar-O_2} + V_{Ar-O}$. V_{O-O_2} is the intramolecular *ab initio* PES of ozone [14]. The high accuracy of the PES was confirmed by the study of rovibrational levels near the dissociation threshold [15] and accounting for the complete permutation symmetry of identical nuclei [16,17], as well as by quantum calculations of isotopic exchange reactions both in stationary [18] and time dependent [19] approaches. V_{ArO_2} and V_{ArO} are the intermolecular *ab initio* PESs built in this Letter. The Ar-O_2 and Ar-O intermolecular PESs were constructed using the unrestricted version of the explicitly correlated single- and double-excitation coupled cluster method with a perturbative treatment of triple excitations [UCCSD(T)-F12a] with the augmented correlation-consistent triple-zeta aug-cc-pVTZ basis set. The final root mean square error of the fit of the *ab initio* data was within 1 cm^{-1} at all energies in the PES potential wells. The constructed PESs have the following configurations of the global minima: $R_e^{Ar-O} = 6.326\ a_0$ (where $a_0 \approx 5.29 \times 10^{-11}$ m is the Bohr radius) and $R_e^{Ar-O_2} = 6.787\ a_0$ ($\alpha = \pi/2$) with the depth of $D_e^{Ar-O_2} = 143.6462$ cm^{-1} (≈ 207 K) and $D_e^{Ar-O} = 90.7967$ cm^{-1} (≈ 131 K), respectively. Potentials are shown in Fig. 1. For more details see Supplemental Material [20].

Dynamics.—Rigorous full quantum scattering calculations for the system are considered as practically unfeasible [25,26]. Various classical calculations [27,28],—statistical [29] or *ad hoc* simplified quantum models and essentially focused on one of the two-step mechanisms,—have been reported [30–33], but a qualitative agreement is still lacking, as reviewed in Refs. [25,26].

The present approach is based on a classical trajectory (CT) method in hyperspherical coordinates, which has shown efficiency for reactive collisions of three neutral atoms [11–13,34] as well as for ion-neutral-neutral ternary recombination processes [35–38]. The method has been adapted to the present problem representing the O_2 molecule as a superatom, thus, reducing the degrees of freedom of the $O + O_2 + Ar$ system. In calculations, it results in a fixed angle between O_2 and the direction to O, corresponding to the bond angle in O_3 (117°). The interaction of Ar with O_3 does not depend significantly on the angle between the plane of $O + O_2$ and the direction to Ar, so to simplify the numerical part of the approach, the angle is fixed to 0. Finally, the angle α between O_2 and Ar is considered a parameter of the problem; Calculations are made for several (8) values of α, and the result is averaged over that parameter. Notice that the average performed in this way does not correspond to when the angular momentum of O_2 is zero because the angular momentum is completely undefined for each given well-defined orientation angle α. Therefore, the averaging procedure corresponds to a wide distribution over angular momenta of O-O_2 relative motion and is appropriate for temperatures significantly larger than the O_2 rotational constant (≈ 2.1 K).

The application of this method to the formation of ozone via ternary recombination reaction $O_2 + O + Ar \rightarrow O_3 + Ar$ is based on the assumption that the internal degrees of freedom of the oxygen molecule do not play an essential role since the excitation of the O_2 vibrational mode requires high collision energy over 1000 cm^{-1} (≈ 1439 K). The assumption can be verified calculating rate coefficients for different bond angles of the ArO_2 molecule, α. As a result, we are able to estimate the uncertainty of the present calculations due to the approximation of the frozen internal degrees of freedom of the oxygen molecule. We have employed 1.3×10^9 trajectories with an appropriate Monte Carlo sampling of the initial conditions for the results reported in this Letter.

Finally, the thermal average of the three-body recombination rate coefficient is obtained by integrating the energy-dependent three-body recombination rate coefficient $k_3(E_c)$ over the appropriate three-body Maxwell-Boltzmann distribution of collision energies E_c, yielding

$$k_3(T) = \frac{1}{2(k_B T)^3} \int_0^\infty k_3(E_c) E_c^2 e^{-E_c/(k_B T)} dE_c, \quad (1)$$

where k_B is the Boltzmann constant and T the temperature of the system.

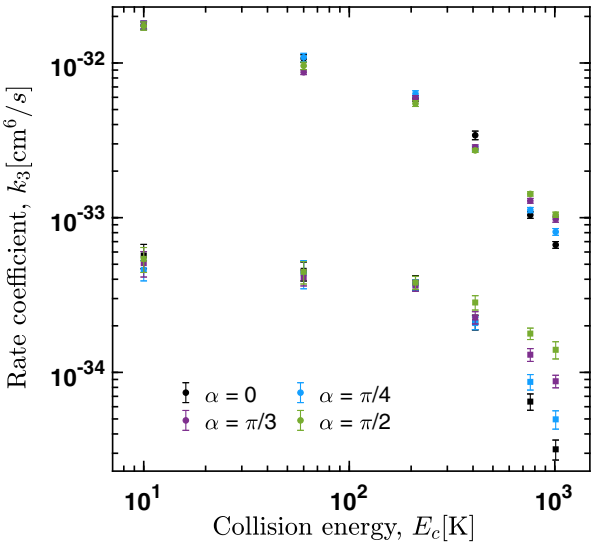

FIG. 2. Energy-dependent recombination rates for O_3 molecules of all binding energies (circles) and those with binding energies > 200 cm^{-1} (squares) for different values of α. The energy (abscissa) is given in temperature units.

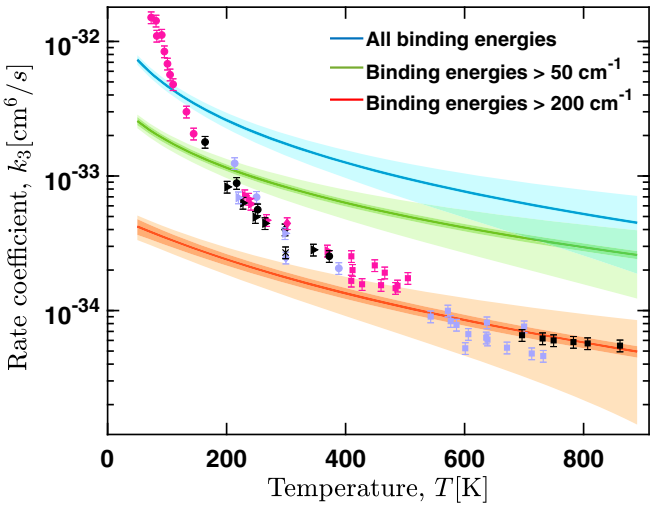

FIG. 3. Thermally averaged recombination rate coefficients for formation of molecules with all binding energies (blue data), with binding energies > 50 cm^{-1} (green data), and with > 200 cm^{-1} (red data). The dark shaded area indicates the statistical error due the stochastic nature of the Monte Carlo technique used in the calculations. The light shaded area shows the confidence interval due to both statistical error and the effect of neglecting explicitly α. Experimental data for $k_3(T)$: magenta circles, Ref. [8]; black circles [7]; cornflower blue circles [39] (scaled to the value at 300 K from Ref. [40]); black triangles [41]; cornflower blue triangles [42]; magenta squares [43] (as cited in Ref. [9]); cornflower blue squares [44]; black squares [45]; cornflower blue diamond [46] (as cited in Ref. [9]); black cross [47]; black diamond [40]; magenta diamond [48]; magenta triangles [49].

Theoretical rate coefficients.—Figure 2 shows the rate coefficient $k_3(E_c, \alpha)$ as function of collision energy obtained for different values of angle α between O_2 and the direction to Ar. Comparing the upper set of data (indicated by circles), which are associated with the ozone molecules of all binding energies, and the lower set (squares), i.e., the formation rates of "deeply bound" levels of O_3 with binding energies larger than 200 cm^{-1} ($\approx$288 K), one can conclude that the majority of molecules formed through ternary recombination are highly excited. Such molecules can be destroyed or stabilized in collisions with other species present in the gas. The cross sections for the two processes are comparable. However, the radiative stabilization is negligible because of the very long radiative lifetimes of these states. Therefore, comparing with an experiment at 300 K, in which only deeply bound or stabilized O_3 molecules are accounted for, one should consider the lower set of data.

Figure 3 gives thermally averaged rate coefficients $k_3(T)$ for molecules with all binding energies and for those with binding energies larger than 50 cm^{-1} ($\approx$72 K) and 200 cm^{-1} ($\approx$288 K) and compares them with available experimental data. Clearly, the theoretical coefficients have different T dependence due to the fact that in an experiment at a given temperature T, only the molecules with binding energies larger than T are collisionally stabilized and accounted for. Indeed, the theoretical data for molecules with binding energies > 50 and > 200 cm^{-1} agree with the experimental data at 70 and 288 K within about 50%.

The role of collisions after formation of highly excited vibrational states of ozone.—To compare the obtained theoretical results with the experimental data more accurately, one would have to account for processes taking place in the experiment once the ternary recombination forms an initial distribution over vibrational levels of O_3, the nascent population. The leading process is the vibrational deexcitation or dissociation of highly excited O_3^* molecules in collisions with other species. A detailed study of process is underway but beyond the scope of this Letter. Here, we will account for the process using a statistical factor $\Delta E/T$, which can be viewed as a survival probability for highly excited O_3^*. It is obtained by integrating cross sections for the stabilization and dissociation processes over the thermal distribution of collisional energies at a given temperature T and computing the ratio of stabilization events to the total number of events (stabilization + dissociation) in such collisions.

The value ΔE is of the order of the energy of Ar-O_3 interaction averaged over involved vibrational states of O_3, which is about 50 cm^{-1} (see the Ar-O and Ar-O_2 curves in Fig. 1). Therefore, we use $\Delta E = 50$ cm^{-1} (70 K). The $\Delta E/T$ dependence is valid only for $T \gtrsim \Delta E$: For lower temperatures, the survival factor is about 1. (Notice that the same dependence for the stabilization factor was suggested by Troe *et al.* [9,50] using a physical kinetics approach). The resulting rate coefficient, accounting for the vibrational

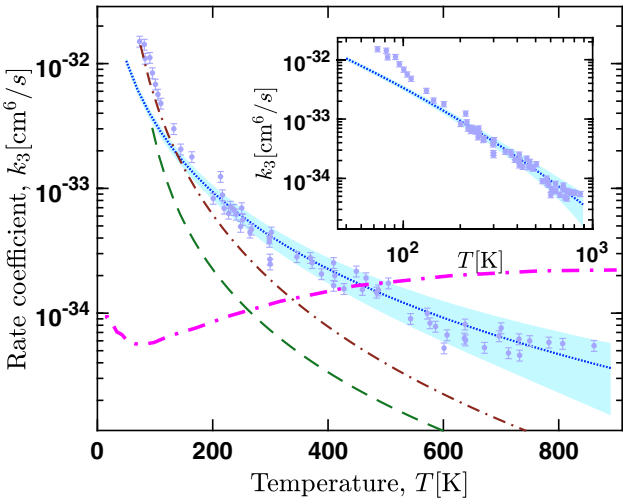

FIG. 4. Thermally averaged recombination rate coefficients for formation of molecules with all binding energies scaled by the factor of 50 cm$^{-1}/T$ accounting for the process of vibrational quenching (solid line). The shaded area (light blue) represents the uncertainty of the theoretical model. The circles with error bars are the same experimental data as in Fig. 3. Previous theoretical results are shown with a thick dash-dotted (magenta) line [30], thin dash-dotted (brown) line [9], and dashed (green) line [28]. The inset shows the data in the log-log scale.

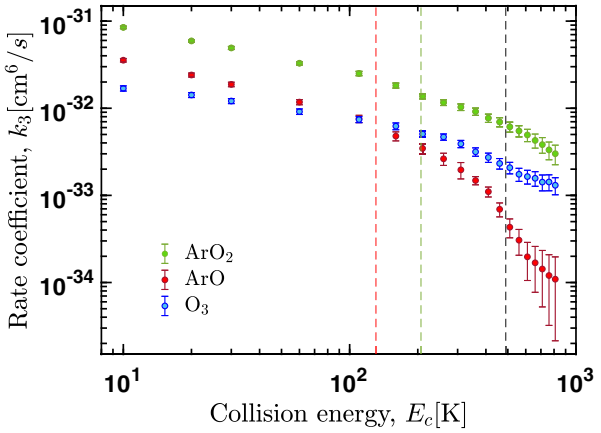

FIG. 5. Ternary recombination rate coefficient $k_3(E_c)$ for formation of the three possible products in the $O + O_2 + Ar$ collisions: O_3, ArO_2, and ArO. Red and green dashed lines indicate the dissociation energies of ArO and ArO_2, respectively. The black dashed line shows the energy related to the shoulder structure of O-O_2.

quenching, is shown in Fig. 4, as well as some previous theoretical approaches for comparison. As one can see, the agreement with experimental data is remarkable for temperatures above 100 K. The good agreement indicates that the main physics of the process is accounted for correctly in the current approach. We would like to point out here that the agreement is sensitive to the value of the parameter ΔE, which—although the same in this study as the one derived by [9]—can have an non-negligible uncertainty, especially at low temperatures, probably, 20%–30%. This adds an additional uncertainty to the theoretical curve in Fig. 4.

Two-step models: Stabilization and Chaperon mechanisms.—The present results allow us to analyze which of the two-step models (stabilization or Chaperon) is dominant. Figure 5 gives the rate coefficients for the formation of all three possible products of the reaction, O_3, ArO_2, and ArO. The figure demonstrates two distinct characteristics: First, at low collision energies ($E_c \lesssim 130$ K) [13,34] ArO_2 is formed more quickly than ArO, which is formed quicker than O_3 (assuming equal densities of Ar, O, and O_2). The result is explained by the fact that the attractive potential of the Ar-O_2 system decays slower than that of Ar-O, so that it has a larger density of available vibrational states to be formed (a larger phase-space volume in the classical formulation of the problem). The same argument applies to the comparison between the O-O_2 and Ar-O potentials.

The second distinct feature in Fig. 5 is the change in the power-law behavior of recombination rates at 200–300 K. The first sudden drop appears in k_3 of ArO around its dissociation energy: At collision energies larger than the dissociation energy, fewer ArO molecules are formed due to higher initial velocities. The rates of formation of ozone and ArO_2 are also affected in a similar way, although in these cases, slopes of the coefficients vary much less than that for ArO. There is another drop in the recombination rates of all products when the collision energy surpasses the dissociation energy of ArO_2. Interestingly, there is another smoother change in the slope of the rate coefficient for O_3 formation that may be due to the shoulder structure on O_3 [14,51], visible in Fig. 1. The overall effect is that for collision energies $\gtrsim$150 K, the probability of forming bound levels of ArO decreases significantly (compared with other products), and the probability of ozone formation overcomes it.

The more significant rate coefficients for the formation of ArO_2 and ArO compared to O_3 at low collision energies mean that the Chaperon mechanism is more important than the stabilization at temperatures $\lesssim$100 K. At higher temperatures, the probability of forming weakly bound ozone molecules is more prominent than for ArO, and hence the stabilization mechanism starts to play a role. Similarly, at even higher temperatures, typical collision energies are larger than binding energies of ArO_2 and ArO, so that formation of the corresponding bound molecules is less likely, and the stabilization mechanism becomes dominant.

Figure 5 shows also previous theoretical results [9,28,30]. Because of a limited space, a detailed discussion—including the models—of the comparison with the present results will be reported in a separate article. Here, we would like only to stress that the previous studies used the two-step approximation to treat the recombination.

Summary.—We would like to stress the following findings of the present study. (1) The rate coefficients for the formation of O_3 in ternary collisions $O + O_2 + Ar$, without

using any two-step approximations, were computed for the first time as a function of collision energies. Thermally averaged coefficients were derived for temperatures 5–900 K. (2) Because of a relatively long observation time in experiments that were performed so far, a direct measurement of the ternary rate coefficient was not possible since the majority of O_3 molecules formed initially, the nascent population, are weakly bound and, therefore, destroyed or stabilized in collisions with other species present in the gas (Ar, O_2, etc.) that affected the observation results. (3) Accounting for the process of vibrational quenching of the nascent population using the survival probability for highly excited O_3^* molecules when colliding with other species leads to a good agreement with available experimental data for temperatures 100–900 K. At temperatures, 50–100 K theory gives smaller rate coefficients. Likely, the classical-trajectory approach is not applicable for these temperatures because, at the corresponding collision energies, details of the resonant structure of O_3 and, possibly, ArO_2 metastable rovibrational states could be important, which cannot be treated accurately using classical-trajectory methods. (4) The rate coefficients obtained in an explicitly three-body approach, without assuming any two-step mechanism, allowed us to conclude that the Chaperon mechanism in ozone formalism is dominant at temperatures below 100 K, while the energy-transfer stabilization mechanism appears to be dominant at $T \gtrsim 700$ K.

This work acknowledges the support from the Tomsk State University and the National Science Foundation, Grant No. 2110279. We also thank Gerard Meijer for his interest and support.

[1] J. Orphal, J. Staehelin, J. Tamminen, G. Braathen, M.-R. De Backer, A. Bais, D. Balis, A. Barbe, P. K. Bhartia, M. Birk *et al.*, J. Mol. Spectrosc. **327**, 105 (2016).
[2] J. Houghton, Y. Ding, D. Griggs, M. Noguer, P. Van der Linden, X. Dai, K. Maskell, and C. Johnson, *Climate Change: The Scientific Basis* (Cambridge University Press, Cambridge, England, 2001), p. 572.
[3] P. W. Barnes, C. E. Williamson, R. M. Lucas, S. A. Robinson, S. Madronich, N. D. Paul, J. F. Bornman, A. F. Bais, B. Sulzberger, S. R. Wilson *et al.*, Nat. Sustainability **2**, 569 (2019).
[4] M. López-Puertas and F. Taylor, *Non-LTE Radiative Transfer in the Atmosphere*, Series on Atmospheric, Oceanic and Planetary Physics (World Scientific, Singapore, 2001).
[5] M. Kaufmann, S. Gil-López, M. López-Puertas, B. Funke, M. García-Comas, N. Glatthor, U. Grabowski, M. Höpfner, G. P. Stiller, T. von Clarmann, M. E. Koukouli, L. Hoffmann, and M. Riese, J. Atmos. Sol. Terr. Phys. **68**, 202 (2006).
[6] A. G. Feofilov and A. A. Kutepov, Surv. Geophys. **33**, 1231 (2012).
[7] H. Hippler, R. Rahn, and J. Troe, J. Chem. Phys. **93**, 6560 (1990).
[8] W. Rawlins, G. Caledonia, and R. Armstrong, J. Chem. Phys. **87**, 5209 (1987).
[9] K. Luther, K. Oum, and J. Troe, Phys. Chem. Chem. Phys. **7**, 2764 (2005).
[10] C. Janssen, J. Guenther, K. Mauersberger, and D. Krankowsky, Phys. Chem. Chem. Phys. **3**, 4718 (2001).
[11] J. Pérez-Ríos, S. Ragole, J. Wang, and C. H. Greene, J. Chem. Phys. **140**, 044307 (2014).
[12] C. H. Greene, P. Giannakeas, and J. Pérez-Ríos, Rev. Mod. Phys. **89**, 035006 (2017).
[13] M. Mirahmadi and J. Pérez-Ríos, J. Chem. Phys. **154**, 034305 (2021).
[14] V. G. Tyuterev, R. V. Kochanov, S. A. Tashkun, F. Holka, and P. G. Szalay, J. Chem. Phys. **139**, 134307 (2013).
[15] V. G. Tyuterev, R. Kochanov, A. Campargue, S. Kassi, D. Mondelain, A. Barbe, E. Starikova, M. R. De Backer, P. G. Szalay, and S. Tashkun, Phys. Rev. Lett. **113**, 143002 (2014).
[16] V. Kokoouline, D. Lapierre, A. Alijah, and V. G. Tyuterev, Phys. Chem. Chem. Phys. **22**, 15885 (2020).
[17] S. Vasilchenko, A. Barbe, E. Starikova, S. Kassi, D. Mondelain, A. Campargue, and V. Tyuterev, Phys. Rev. A **102**, 052804 (2020).
[18] P. Honvault, G. Guillon, R. Kochanov, and V. Tyuterev, J. Chem. Phys. **149**, 214304 (2018).
[19] C. H. Yuen, D. Lapierre, F. Gatti, V. Kokoouline, and V. G. Tyuterev, J. Phys. Chem. A **123**, 7733 (2019).
[20] See Supplemental Material at http://link.aps.org/supplemental/10.1103/PhysRevLett.128.108501 for more details on the PES as well as on the classical trajectory method, which includes Refs. [21–24].
[21] J. Pérez-Ríos, *An Introduction to Cold and Ultracold Chemistry* (Springer International Publishing, New York, 2020).
[22] L. F. Shampine and M. W. Reichelt, SIAM J. Sci. Comput **18**, 1 (1997).
[23] R. Ashino, M. Nagase, and R. Vaillancourt, Comput. Math. Appl. **40**, 491 (2000).
[24] L. F. Shampine, Comput. Math. Appl. **44**, 749 (2002).
[25] R. Schinke, S. Y. Grebenshchikov, M. Ivanov, and P. Fleurat-Lessard, Annu. Rev. Phys. Chem. **57**, 625 (2006).
[26] A. Teplukhin and D. Babikov, Phys. Chem. Chem. Phys. **18**, 19194 (2016).
[27] R. Schinke and P. Fleurat-Lessard, J. Chem. Phys. **122**, 094317 (2005).
[28] M. V. Ivanov and R. Schinke, J. Chem. Phys. **124**, 104303 (2006).
[29] Y. Q. Gao and R. Marcus, Science **293**, 259 (2001).
[30] D. Charlo and D. C. Clary, J. Chem. Phys. **120**, 2700 (2004).
[31] T. Xie and J. M. Bowman, Chem. Phys. Lett. **412**, 131 (2005).
[32] S. Y. Grebenshchikov and R. Schinke, J. Chem. Phys. **131**, 181103 (2009).
[33] A. Teplukhin and D. Babikov, Faraday Discuss. **212**, 259 (2018).
[34] M. Mirahmadi and J. Pérez-Ríos, J. Chem. Phys. **155**, 094306 (2021).

[35] J. Pérez-Ríos and C. H. Greene, J. Chem. Phys. **143**, 041105 (2015).
[36] A. Krükow, A. Mohammadi, A. Härter, J. H. Denschlag, J. Pérez-Ríos, and C. H. Greene, Phys. Rev. Lett. **116**, 193201 (2016).
[37] J. Pérez-Ríos and C. H. Greene, Phys. Rev. A **98**, 062707 (2018).
[38] J. Pérez-Ríos, Mol. Phys. **119**, e1881637 (2021).
[39] M. Mulcahy and D. Williams, Trans. Faraday Soc. **64**, 59 (1968).
[40] F. Kaufman and J. R. Kelso, J. Chem. Phys. **46**, 4541 (1967).
[41] R. E. Huie, J. T. Herron, and D. D. Davis, J. Phys. Chem. **76**, 2653 (1972).
[42] I. Arnold and F. Comes, Chem. Phys. **42**, 231 (1979).
[43] E. Intezarova and V. Kondratiev, Izv. Akad. Nauk. SSSR, Ser. Khim. **11**, 2440 (1967).
[44] C. Park, J. Phys. Chem. **81**, 499 (1977).
[45] M. C. Sauer Jr. and L. M. Dorfman, J. Am. Chem. Soc. **87**, 3801 (1965).
[46] R. Center and R. Kung, J. Chem. Phys. **62**, 802 (1975).
[47] P. Bevan and G. Johnson, J. Chem. Soc., Faraday Trans. 1 F **69**, 216 (1973).
[48] T. Slanger and G. Black, J. Chem. Phys. **53**, 3717 (1970).
[49] O. Klais, P. C. Anderson, and M. J. Kurylo, Int. J. Chem. Kinet. **12**, 469 (1980).
[50] J. Troe, J. Chem. Phys. **66**, 4745 (1977).
[51] D. Lapierre, A. Alijah, R. Kochanov, V. Kokoouline, and V. Tyuterev, Phys. Rev. A **94**, 042514 (2016).